A green approach to magnetically-hard electrically-conducting polyaniline/$CoFe_2O_4$ nanocomposites

Cristina Della Pina,[a] Anna Maria Ferretti,[b] Alessandro Ponti,[b,*] Ermelinda Falletta[a,*]

[a] Dipartimento di Chimica, Università degli Studi di Milano, e ISTM-CNR, Via C. Golgi, 19 - 20133 - Milano (Italy), e-mail: cristina.dellapina@unimi.it, ermelinda.falletta@unimi.it

[b] Laboratorio di Nanotecnologie, Istituto di Scienze e Tecnologie Molecolari, Consiglio Nazionale delle Ricerche, Via G. Fantoli, 16/15 - 20138 - Milano (Italy), e-mail: anna.ferretti@istm.cnr.it, alessandro.ponti@istm.cnr.it

Corresponding authors. Ermelinda Falletta, Dipartimento di Chimica, Università degli Studi di Milano, Via C. Golgi, 19 - 20133 - Milano (Italy), Tel: +39 0250314410, ermelinda.falletta@unimi.it. Alessandro Ponti, Istituto di Scienze e Tecnologie Molecolari, Consiglio Nazionale delle Ricerche, Via C. Golgi, 19 - 20133 - Milano (Italy), Tel: +39 0250314280, alessandro.ponti@istm.cnr.it

Abstract

Magnetically-hard, electrically-conducting polyaniline/$CoFe_2O_4$ nanocomposites were prepared by ~~one-pot~~ oxidative polymerization of *N*-(4-aminophenyl)aniline using molecular oxygen or hydrogen peroxide as the oxidants and magnetic $CoFe_2O_4$ nanoparticles, both uncoated and oleic acid-coated, with the double role of polymerization catalyst and magnetic filler. Oleic acid-coated nanoparticles showed higher catalytic activity than uncoated ones, especially under aerobic conditions. The size of the nanoparticles did not undergo significant changes during the polymerization process. The nanocomposites are magnetically hard with large remanence/saturation ratio, very large coercivity (8–15 kOe at 5 K) and do not display superparamagnetic effects even at RT. The addition of Fe^{3+} as a further oxidant allowed to tune the

electroconductive properties of the materials, with conductivity ranging from $7.3 \cdot 10^{-5}$ S/cm to $5.5 \cdot 10^{-3}$ S/cm.

Keywords: A. Nano composites, A. Nano particles, A. Polymer-matrix composites (PMCs), B. Magnetic properties, Polyaniline.

1. Introduction

Nanocomposite materials combining an electrically conducting polymer (ECP) and magnetic nanoparticles (NPs) have been intensively investigated for their fascinating application as electrochromic devices, [1, 2] electromagnetic interference shields, [3, 4] non-linear optical systems, [5] and microwave absorbers. [6] Among ECPs, polyaniline (PANI) is particularly interesting for its high conductivity, easy synthesis, low cost, and good environmental stability, which make it a promising candidate for many applications. PANI is unique for its tunable electrical conductivity. Among the forms that PANI can assume (reduced leucoemeraldine, half-oxidized emeraldine and oxidized pernigraniline), only the half-oxidized, half-protonated emeraldine salt is electrically conductive. In general, PANI/magnetic-NP composites are prepared by multi-step approaches involving separate NP synthesis and aniline polymerization. The latter requires strong stoichiometric oxidants, such as $(NH_4)_2S_2O_8$ or metal ions in high oxidation state [7], and the resulting inorganic by-products represent a serious drawback related to waste management [8]. Up to now, PANI/$CoFe_2O_4$ nanocomposites were prepared by these approaches. [9-19] They comprised PANI in the conductive form and were only moderately hard [9-13] despite $CoFe_2O_4$ is the magnetically hardest cubic ferrite. Applications as EMI shielding materials, [10, 11, 13] photocatalysts, [14, 16] bactericides, [17, 18] and supercapacitors [19] were demonstrated.

Recently, we reported on the use of eco-friendly oxidants, such as O_2 and H_2O_2, with the aid of suitable catalysts as a “green” alternative to produce ECPs. [20-24] In particular, Fe_3O_4 NPs resulted to be active catalysts in the oxidative polymerization of N-(4-

aminophenyl)aniline (aniline dimer, AD), leading to electrically conductive, superparamagnetic PANI/Fe_3O_4 nanocomposites. [24] We herein report on the behavior of $CoFe_2O_4$ NPs as a polymerization catalyst and magnetic nano-filler for the preparation of PANI/$CoFe_2O_4$ nanocomposites. $CoFe_2O_4$ NPs were proven to be an effective catalyst allowing to achieve magnetically hard nanocomposites with high magnetization and coercivity. The electrical conductivity of the nanocomposites could be tuned by adding a further environmentally-friendly oxidant.

2. Material and methods

2.1. Reagents and instruments

All chemicals were used as received without any purification. FT-IR spectra (400-4000 cm^{-1}) were recorded by a JASCO FT/IR-410 spectrophotometer using pellets of samples dispersed 1:100 w/w in KBr. UV-Vis spectra were recorded on a Hewlett Packard 8453 spectrophotometer using 0.087-0.353 mM solutions in *N*,*N*-dimethylformamide. For transmission electron microscopy (TEM, Zeiss LIBRA-200FE), a drop of NP dispersion (toluene) or nanocomposite suspension (acetonitrile) was evaporated on a carbon-film grid. Powder X-ray diffraction (XRD) patterns were recorded using a Rigaku D IIIMAX horizontal-scan powder diffractometer with Cu K_α radiation. The metal content of the NPs and nanocomposites was determined by atomic absorption spectroscopy (AAS) on a AAS 3100 PerkinElmer spectrophotometer after sample mineralization in aqua regia. EDS (Energy Dispersive X-ray Spectroscopy) characterization was carried out on a Hitachi TM1000 SEM microscope. The electrical conductivity was measured by an AMEL 338 multimeter as detailed in Sec. 2.5. A Quantum Design MPMS XL-5 SQUID magnetometer was used to measure the magnetic properties of NPs and nanocomposites as detailed below (Sec 2.3.6).

2.2. Preparation of $CoFe_2O_4$ NPs

2.2.1. Preparation of uncoated $CoFe_2O_4$ NPs. According to the method of Kang, [25] aqueous solutions of $FeCl_3 \cdot 6H_2O$ (0.30 M, solution A) and $CoCl_2 \cdot 6H_2O$ (0.15 M,

solution B) were prepared dissolving the appropriate amount of salts in 0.4 M aq. HCl. 10 mL of each solution (Fe/Co = 2, atomic ratio) were mixed and stirred for 20 minutes at 80°C under nitrogen. Then, 1.5 M aq. NaOH was quickly added until reaching pH 13 under vigorous stirring. After 2 hours the product was magnetically decanted, washed repeatedly with distilled water until neutral pH and dried at 70°C in oven (yield 91 %).

2.2.2. Preparation of oleic acid-coated (OAC) $CoFe_2O_4$ NPs. Oleic acid (0.2 g) was added to dried uncoated $CoFe_2O_4$ NPs (0.75 g) and stirred in 63 mL of toluene to obtain a uniform suspension. The concentration of $CoFe_2O_4$ in the suspension was measured by AAS (11.9 $mg_{CoFe2O4}$/ml).

2.3. Synthesis of PANI/$CoFe_2O_4$ nanocomposites

2.3.1.Oxidative polymerization reaction by molecular oxygen. 460 mg (2.5 mmol) of *N*-(4-aminophenyl)aniline (AD) were dissolved in 40 mL of 0.03 M aq. HCl. Different amounts of uncoated or OAC $CoFe_2O_4$ NPs were added (AD/$CoFe_2O_4$ = 5, 10, 50 molar ratio). The suspension was stirred under molecular oxygen (p_{O2} = 2 bar) for 72 hours at 80°C. The resulting dark solid was collected by filtration, washed with water and acetone and dried at 383 K overnight. A blank test was repeated in the absence of $CoFe_2O_4$ NPs and no solid product was obtained.

2.3.2. Oxidative polymerization reaction by hydrogen peroxide. 460 mg of AD (2.5 mmol) were dissolved in 40 mL 0.03 M aq. HCl. Different amounts of uncoated or OAC $CoFe_2O_4$ NPs (AD/$CoFe_2O_4$ = 5, 10, 50 molar ratio) and 0.77 mL of aq. H_2O_2 (30%, w/w) were added (H_2O_2/AD = 3, molar ratio). The reaction mixture was stirred at RT for 24 hours. The product was collected by filtration and treated as above (section 2.3.1). The reaction was repeated in the absence of $CoFe_2O_4$ NPs and, as previously reported, [21, 24] a green solid material, identified as emeraldine salt (ES), was obtained (sample 1).

2.3.3. Oxidative polymerization reaction by hydrogen peroxide and Fe^{3+} ~~as co-catalyst~~. The reactions were carried out as described in section 2.3.2 in the presence of $CoFe_2O_4$ NPs and adding $FeCl_3$ (AD/Fe = 1000, molar ratio) into the mixture (sample 11).

2.4. Synthesis of leucoemeraldine

Leucoemeraldine was prepared as described in ref. [26]. 1 g of sample 1 was de-doped with 20 mL of 1.5 M aq. NaOH, obtaining emeraldine base (EB). The latter was filtered and washed with water until neutrality of the mother liquors. 300 mg of EB were dispersed in 5 mL of aq. hydrazine (35%). After 5 hours the product was filtered, washed with acetone, dried under vacuum and stored under nitrogen (sample 2).

2.5. Conductivity measurements

For conductivity measurement, 200 mg of finely powdered sample (ES (sample 1), leucoemeraldine (sample 2), and PANI/$CoFe_2O_4$ nanocomposites) were pressed between 13 mm anvils with force 10 ton for 30 minutes. The resulting disk was next pressed with force 2 kg for 30 minutes. Resistance R was measured by an AMEL 338 multimetre and conductivity σ was obtained as

$$\sigma = (1/R)\,(\ell/A) \qquad (1)$$

where ℓ is the thickness of the disk, R is the resistance and A is the area of the disk base.

2.6. Magnetic measurements

Weighted amounts of powdered samples were packed in Teflon ribbon and set in the magnetometer sample space. Magnetization isotherms $M(H)$ were measured between +50 and –50 kOe at 5 K after field cooling (FC, H_{cool} = +50 kOe) from 295 K. The temperature dependence of the magnetization $M(T)$ was measured between 5 and 300 K using a measuring field H_{meas} = 10 Oe in both zero-field cooling (ZFC) and FC (H_{cool} = 10 Oe) modes. The raw data were corrected for diamagnetic contributions.

3. Results and Discussion

3.1. Catalytic polymerization of AD

As demonstrated by Wei *et al*., [27] owing to the higher oxidation potential of aniline with respect to AD, the slowest step of polyaniline synthesis consists in the aniline monomer oxidation into AD. Recently, we demonstrated that this kinetic bottleneck can be overcome by using AD as reagent since it can be easily polymerized by mild

oxidants (H_2O_2 or O_2) in the presence of suitable catalysts. [23, 24] As previously observed by us for Fe_3O_4 NPs, [24] both uncoated and OAC $CoFe_2O_4$ NPs exhibited catalytic activity (Table 1). The reaction yield was calculated according to Equation 2:

$$\text{Yield}\% = (\Sigma_{\text{mass insoluble materials}} / \Sigma_{\text{mass reagent}}) \times 100 \quad (2)$$

where $\Sigma_{\text{mass reagent}}$ = AD+HCl+$CoFe_2O_4$+oleic acid. To compare the NP activity between reactions involving O_2 or H_2O_2, it is useful to subtract from the yield of the reaction carried out in the presence of H_2O_2 the yield observed in the same conditions but in the absence of NPs, as the latter arises from NP-independent polymerization. Considering the yield values in brackets in Table 1, it is clear that the NPs resulted to be more active under aerobic conditions than in the presence of H_2O_2, in agreement with literature. [8] Furthermore, whereas similar catalytic activity was observed for both $CoFe_2O_4$ NPs types using O_2, in the presence of H_2O_2 OAC NPs exhibited higher catalytic performances than uncoated NPs. This behavior could be ascribed to the ability of cubic ferrites (in particular, $MnFe_2O_4$ and $CoFe_2O_4$) to decompose H_2O_2, [28] decreasing the oxidant concentration in the reaction mixture and thus producing polymer in lower yield. The coating of OAC NPs probably reduces the H_2O_2-NP interaction thereby leading to higher yields (Table 1). In order to exclude any catalyst leaching, the inorganic content of the nanocomposites was analyzed by AAS and EDS. The results confirmed that $CoFe_2O_4$ NPs were mostly incorporated in the insoluble nanocomposites with no change of Fe/Co ratio. This suggests that $CoFe_2O_4$ NPs acted as a true heterogeneous catalyst since their performance cannot be attributed to corrosion phenomena in solution. We conclude this section by comparing the present results with those obtained using Fe_3O_4 NPs. [24] $CoFe_2O_4$ NPs are more active than Fe_3O_4 NPs by about 10% in yield when uncoated NPs are compared, irrespective of the used oxidant; the reverse occurs for OAC NPs. Both Fe_3O_4 and $CoFe_2O_4$ NPs are more active when used in conjunction with O_2, provided that NP-catalyzed yield only is considered. The higher yield for OAC *vs*. uncoated NPs when H_2O_2 is used was not observed for Fe_3O_4 NPs, which are less effective in decomposing H_2O_2. Hence, similar polymer yield can

be obtained by a suitable choice of NP coating and oxidant that compensates for replacing Fe^{2+} with Co^{2+} in the ferrite structure.

3.2. Spectroscopic characterization

$CoFe_2O_4$ NPs were characterized by XRD, TEM, AAS, and EDS. The diffractogram in Figure 1a corresponds to the cobalt ferrite phase with cubic spinel structure. [29] This diffractogram was analyzed by the Rietveld method as implemented in the MAUD software [30] to evaluate the crystallite size. The sample was modeled as a collection of randomly-oriented $CoFe_2O_4$ NPs with log-normal size distribution. The best-fit mean crystallite size was D_{XRD} = 16.0(4) nm. Electron diffraction (Figure 1b) confirmed that the NPs are crystalline, have spinel structure, and are randomly oriented. TEM images (Figure 1c,d) revealed that $CoFe_2O_4$ NPs formed agglomerates even after treatment with oleic acid. The individual NPs range in size from 3 to 25 nm, in reasonable agreement with the D_{XRD}, showing that the NPs are single crystals. The smaller NPs have spheroidal shape while the larger ones appear polygonal in the TEM images. The Fe/Co molar ratio, measured by AAS and EDS in two different $CoFe_2O_4$ NPs batches for each preparation type, was in good agreement with the stoichiometric ratio (Fe/Co = 2). In fact, for uncoated NPs the Fe/Co atomic ratio measured by AAS (EDS) resulted to be 1.96 (1.92) and 2.11 (1.90) for the first and second batch, respectively. Similarly, for OAC NPs it was 1.98 (1.95) for the first batch and 2.08 (1.97) for the second one.

The XRD patterns of PANI/$CoFe_2O_4$ nanocomposites (Figure 1a) revealed the presence of $CoFe_2O_4$ NPs inside the PANI matrix. Rietveld analysis showed that the mean crystallite size of $CoFe_2O_4$ NPs did not significantly change during polymerization [D_{XRD} = 16.1(4) nm for sample 9^{unc} and 15(6) nm for sample 10^{unc}]. Since uncoated and OAC $CoFe_2O_4$ NPs led to very similar patterns, we decided to limit FT-IR and UV-Vis spectroscopic investigations to the nanocomposites obtained using uncoated NPs. The PANI matrix of the nanocomposites was characterized by FT-IR and UV-Vis spectroscopy (Figure 2). The ratio between the FT-IR bands at 1570 cm^{-1} (quinoid band, Q) and 1498 cm^{-1} (benzenoid band, B), as well as the intensity of the band at *ca.* 1144

cm^{-1} (electronic-like band) are strictly related to the conductive behavior of the polymer. [31] The Q/B intensity ratio (Table 2) gradually decreases passing from sample 1 to 6^{unc} and 2 showing that PANI in nanocomposite 6^{unc} has intermediate oxidation state between the half-oxidized emeraldine salt (sample 1) and reduced leucoemeraldine (sample 2). Moreover, the electronic-like band, typical of conducting emeraldine form, is very strong for sample 1, weak for sample 2, and again intermediate for nanocomposite 6^{unc} (see Figure 2). UV-Vis spectroscopy confirmed these observations. All the UV-Vis spectra reported in Figure 2 showed two characteristic broad bands, at *ca.* 300 nm (band 1) and *ca*. 600 nm (band 2). Band 1 is associated with a π-π* transition of the conjugated ring system, whereas band 2 can be assigned to a benzenoid to quinoid excitonic transition. [32, 33] Therefore, the intensity ratio of the two bands indicates the oxidation state of PANI. [34] Table 2 summarizes the UV-Vis spectroscopic parameters (wavelength of band maximum, λ, and molar extinction coefficient, ε). The $\varepsilon_1/\varepsilon_2$ ratio increases passing from sample 1 to 6^{unc} and 2 thus confirming that PANI in nanocomposite 6^{unc} has intermediate oxidation state. The spectroscopic characterization clearly show that Fe_3O_4 [24] and $CoFe_2O_4$ NPs led to different oxidation states of PANI matrix, despite exhibiting similar catalytic behavior in the oxidative polymerization of AD. Accordingly, Fe_3O_4 NPs yielded nanocomposites comprising PANI in its conductive emeraldine form, whereas $CoFe_2O_4$ NPs led to nanocomposites featuring a more reduced PANI matrix.

Even though reduced PANI forms find application in several areas, such as electrochromic devices and Li-PANI batteries, [35] emeraldine salt is the most investigated and used form of PANI. While investigating PANI/$CoFe_2O_4$ nanocomposites, we found that the addition of Fe^{3+}, a cation able to complete the oxidation process, [23] allowed us to obtain nanocomposites (sample 11) containing conductive emeraldine salt, as confirmed by FT-IR and UV-vis spectroscopy. Indeed, nanocomposite 11 presents FT-IR (Q/B = 0.99, strong electronic-like band) and UV-Vis ($\varepsilon_1/\varepsilon_2$ = 1.82) spectra close to those observed for emeraldine salt (sample 1).

3.3. Conductivity measurements

The conductivity values of sample 1 (emeraldine salt), sample 2 (leucoemeraldine) and PANI/$CoFe_2O_4$ nanocomposites (samples 6^{unc} and 11) are in good agreement with FT-IR and UV-Vis results. As expected, PANI/$CoFe_2O_4$ nanocomposites (sample 9^{OAC} and 10^{OAC}) displayed a conductivity ($7.3\cdot10^{-5}$ and $4.9\cdot10^{-5}$ S/cm) intermediate between sample 1 ($3.5\cdot10^{-3}$ S/cm) and sample 2 ($1\cdot10^{-8}$ S/cm). However, the nanocomposite synthesized in the presence of Fe^{3+} (sample 11) exhibited a conductivity of $5.5\cdot10^{-3}$ S/cm, very similar to the value obtained for sample 1 and comparable to those reported for PANI/Fe_3O_4 nanocomposites. [24] The conductivity of emeraldine salt prepared by AD oxidative polymerization was found to be lower than that of PANI prepared from aniline (typically 4.4 S/cm). [36] This is in agreement with the pioneering investigations of Kitani and Geniès [37, 38] who attributed such behavior to the different length of the polymeric chains, which are shorter in PANI from AD than in traditional PANI.

3.4 Magnetic properties

The ZFC/FC and isothermal magnetization curves of OAC $CoFe_2O_4$ NPs and related nanocomposites are shown in Fig. 3. The principal magnetic parameters are reported in Table 3. The ZFC/FC curves of OAC $CoFe_2O_4$ NPs overlap in the 5-300 K range and both M_{ZFC} and M_{FC} increase on cooling, similarly to bulk ferrites. [39] Although some of the NPs are expected to be superparamagnetic (SPM) since the blocking diameter for non-interacting $CoFe_2O_4$ NPs is 9 nm at 300 K and 2 nm at 5 K, [40] there is no evidence of SPM behavior with its characteristic FC-ZFC bifurcation and blocking-unblocking processes. [41] To confirm that the magnetization has bulk-like behavior, we fitted the M_{FC} data to a generalized form of the Bloch $T^{3/2}$ law [42]

$$M(T) = M(0)\,[1 - (T/T_0)^b]. \qquad (3)$$

The experimental data could be very well fitted to the model. The best-fit parameters $b = 1.91\pm0.01$ and $T_0 = (746\pm3)$ K are close to the bulk $CoFe_2O_4$ values, *i. e.*, $b_{bulk} = 2$ and $T_{0,bulk} = 797$ K. [42] Our T_0 value is different from those obtained for

solvothermally produced 3-11 nm $CoFe_2O_4$ NPs (1100-1500 K), which have strong surface effects. [42] The low-field behavior of OAC $CoFe_2O_4$ NPs is thus close to that of random-anisotropy polycrystalline bulk $CoFe_2O_4$, without significant SPM or surface effects. The individual $CoFe_2O_4$ nanocrystals are strongly coupled by inter-particle exchange interaction, which are effective since the NPs are in direct contact, as shown by TEM images. Similar conclusions can be drawn for the nanocomposites, which have similar ZFC/FC magnetization curves and b, T_0 parameters. Partial SPM behavior is observed for sample 9^{OAC} which shows the typical increase of M_{ZFC} between 5 and 60 K due to thermal unblocking of magnetization and, less clearly, for 6^{OAC} where the thermal unblocking occurs between 250 and 300 K.

The maximum-field magnetization M_{sat} observed in the FC isothermal magnetization curves of the OAC $CoFe_2O_4$ NPs and nanocomposites synthesized with O_2 is less than the bulk $CoFe_2O_4$ value (93.9 emu/g at 5 K), a behavior commonly observed in ferrite nanoparticles and attributed to intrinsic surface-related effects. [43] Unexpectedly, nanocomposites synthesized with H_2O_2 have large M_{sat}, even higher than the bulk value. This behavior cannot be attributed to the presence of impurities since (i) XRD ruled out inorganic phases with non-spinel structure and (ii) impurities with spinel structure cannot increase M_{sat} as Co_3O_4 is antiferromagnetic at 5 K [44] and Fe_3O_4 has a low-temperature saturation magnetization of 98 emu/g. [45] Therefore, the increasing trend of M_{sat} with decreasing NP content is related to $CoFe_2O_4$ NPs and suggests that inter-particle interactions play a role in the reduction of M_{sat}. Such interactions probably are of magnetostatic origin since exchange interaction enhances magnetization by competing against the random-axis anisotropy. [46] Concentration dependence is clearly revealed by the M_{rem}/M_{sat} ratio (see Table 3). The M_{rem}/M_{sat} ratio of OAC $CoFe_2O_4$ NPs is unusually higher than the value 0.5 generally accepted for NPs and not far from the value 0.832 calculated for cubic Stoner-Wohlfarth NPs with iron-type ($K_1 > 0$) anisotropy. [47] The M_{rem}/M_{sat} ratio is lower in nanocomposites, mainly because of the increase of M_{sat} at lower NP content, but still in the 0.25-0.5 range.

A dependence on the $CoFe_2O_4$ content is also observed for coercivity H_c. OAC $CoFe_2O_4$ NPs have a very high coercivity at 5 K, which is a sizeable fraction of the coercivity $H_{c0} = 0.479\ H_{an} \cong 39$ kOe predicted for randomly-oriented Stoner-Wohlfarth $CoFe_2O_4$ NPs at 5 K, where $H_{an} = 2K_1/M_{sat}$ is the anisotropy field. Similarly large coercivity has been reported for aggregated $CoFe_2O_4$ NPs. [48, 49] Such a coercivity and the absence of SPM even at low field can be explained by an effective exchange coupling between NPs in direct contact. In this case, coercivity reduction can be expressed as [46]

$$H_c \cong H_{an}\,(D/\delta)^6\,, \qquad (4)$$

where D is the NP size and $\delta \cong 20$ nm is the $CoFe_2O_4$ Bloch wall width. [40] Inserting the experimental value $H_c = 18.2$ kOe, one obtains $D \cong 16$ nm, in good agreement with XRD and TEM data. In summary, OAC $CoFe_2O_4$ NPs behave as Stoner-Wohlfarth NPs with reduced coercivity due to inter-particle exchange interaction in the medium coupling limit where D is comparable to δ. The coercivity of nanocomposites is smaller but still very high and their H_{cr} values are at most 10% lower than that of the pure NPs, showing that the nanocomposites are magnetically hard and retain the barrier to irreversible magnetization inversion of the pure NPs. The coercivity decrease in the nanocomposites is explained by assuming that some aggregates were separated in smaller fragments during polymerization, as probably occurred in sample 9^{OAC} that shows blocking-unblocking behavior at low field.

A comparison with similarly synthesized PANI/Fe_3O_4 nanocomposites [24] is of interest. PANI/$CoFe_2O_4$ nanocomposites have similar M_{sat} and M_{rem} (referred to composite mass) and about 100-fold larger coercivity with respect to PANI/Fe_3O_4 nanocomposites, thus demonstrating that the former are magnetically much harder. A curious behavior shared by these nanocomposites is the large M_{sat} observed when the oxidant is O_2. M_{sat} is even larger than in the case of pure NPs and close to (sometimes larger than) the bulk value. With respect to those previously reported, [9-13] our PANI/$CoFe_2O_4$ nanocomposites have higher coercivity. Only two nanocomposites

described in Ref. [12] have comparable coercivity (≈ 10 kOe) but display lower M_{sat} than the present nanocomposites. In this case, in fact, the presence of PANI increases M_{sat} whereas it decreases M_{sat} in the nanocomposites of Ref. [12]. In summary, our PANI/$CoFe_2O_4$ nanocomposites are magnetically harder than those previously reported.

4. Conclusions

The catalytic behavior of $CoFe_2O_4$ NPs in the oxidative polymerization of *N*-(4-aminophenyl)aniline to polyaniline is herein described for the first time. $CoFe_2O_4$ NPs have good catalytic activity, especially when OAC NPs are used. At variance with previously reported cases, [9-19] the PANI matrix of the nanocomposites is obtained in an intermediate oxidation state between emeraldine and leucoemeraldine. However, the addition of Fe^{3+} as further oxidant induces the formation of PANI/$CoFe_2O_4$ nanocomposites where PANI is in the conducting emeraldine form. The magnetic behavior of the $CoFe_2O_4$ nano-filler is dominated by the interparticle exchange interaction that overshadows size and surface effects. The nanocomposites are magnetically hard and have high specific magnetization and coercivity. In summary, our PANI/$CoFe_2O_4$ nanocomposites bear the following advantages: (i) environmentally friendly synthesis, (ii) high coercivity, and (iii) tunable electrical conductivity. The high polymerization yield attainable with both $CoFe_2O_4$ and Fe_3O_4 NPs (provided suitable NP coating and oxidant are selected) and the ability to tune the PANI/$CoFe_2O_4$ electrical conductivity allow one to prepare PANI/ferrite nanocomposites with desired electrical and magnetic properties to meet the demand of the considered application.

Acknowledgments

The authors gratefully acknowledge financial support by Fondazione Cariplo (Milano, Italy) under grant n. 2012-0872 (Magnetic-nanoparticle-filled conductive polymer composites for EMI reduction). AMF and AP gratefully acknowledge financial support by the Italian MIUR under grant FIRB RBAP115AYN (Oxides at the nanoscale: multifunctionality and applications).

References

[1] Wang XH, Shao MW, Shao G, Wu ZC, Wang SW. A facile route to ultra-long polyaniline nanowires and the fabrication of photoswitch. J Colloid Interface Sci. 2009;332(1):74-77.

[2] Shen PK, Huang HT, Tseung ACC. A Study of Tungsten Trioxide and Polyaniline Composite Films .1. Electrochemical and Electrochromic Behavior. J Electrochem Soc. 1992;139(7):1840-1845.

[3] Guskos N, Anagnostakis EA, Likodimos V, Bodziony T, Typek J, Maryniak M, et al. Ferromagnetic resonance and ac conductivity of a polymer composite of Fe_3O_4 and Fe_3C nanoparticles dispersed in a graphite matrix. J Appl Phys. 2005;97(2).

[4] Miyauchi S, Abiko H, Sorimachi Y, Tsubata I. Preparation of Barium-Titanate Polypyrrole Compositions and Their Electrical-Properties. J Appl Polym Sci. 1989;37(1):289-293.

[5] Peng XG, Zhang Y, Yang J, Zou BS, Xiao LZ, Li TJ. Formation of Nanoparticulate Fe_2O_3-Stearate Multilayer through the Langmuir-Blodgett Method. J Phys Chem. 1992;96(8):3412-3415.

[6] Makeiff DA, Huber T. Microwave absorption by polyaniline-carbon nanotube composites. Synth Met. 2006;156(7-8):497-505.

[7] Mallick K, Witcomb MJ, Dinsmore A, Scurrell MS. Fabrication of a metal nanoparticles and polymer nanofibers composite material by an in situ chemical synthetic route. Langmuir. 2005;21(17):7964-7967.

[8] Sun ZC, Geng YH, Li J, Wang XH, Jing XB, Wang FS. Catalytic oxidization polymerization of aniline in an H_2O_2-Fe^{2+} system. J Appl Polym Sci. 1999;72(8):1077-1084.

[9] Ding H, Liu X-M, Wan M, Fu S-Y. Electromagnetic functionalized cage-like polyaniline composite nanostructures. J Phys Chem B. 2008;112(31):9289-9294.

[10] Su B-T, Zuo X-W, Hu C-L, Lei Z-Q. Synthesis and Electromagnetic Properties of Polyaniline/$CoFe_2O_4$ Nanocomposite. Acta Phys-Chim Sin. 2008;24(10):1932-1936.

[11] Gandhi N, Singh K, Ohlan A, Singh DP, Dhawan SK. Thermal, dielectric and microwave absorption properties of polyaniline-$CoFe_2O_4$ nanocomposites. Compos Sci Technol. 2011;71(15):1754-1760.

[12] Prasanna GD, Jayanna HS, Lamani AR, Dash S. Polyaniline/CoFe2O4 nanocomposites: A novel synthesis, characterization and magnetic properties. Synth Met. 2011;161(21-22):2306-2311.

[13] Chen K, Xiang C, Li L, Qian H, Xiao Q, Xu F. A novel ternary composite: fabrication, performance and application of expanded graphite/polyaniline/$CoFe_2O_4$ ferrite. J Mater Chem. 2012;22(13):6449-6455.

[14] Xiong P, Chen Q, He M, Sun X, Wang X. Cobalt ferrite-polyaniline heteroarchitecture: a magnetically recyclable photocatalyst with highly enhanced performances. J Mater Chem. 2012;22(34):17485-17493.

[15] Leng C, Wei J, Liu Z, Xiong R, Pan C, Shi J. Facile synthesis of PANI-modified $CoFe_2O_4$-TiO_2 hierarchical flower-like nanoarchitectures with high photocatalytic activity. J Nanopart Res. 2013;15(5):1643.

[16] Xiong P, Wang L, Sun X, Xu B, Wang X. Ternary Titania-Cobalt Ferrite-Polyaniline Nanocomposite: A Magnetically Recyclable Hybrid for Adsorption and Photodegradation of Dyes under Visible Light. Ind Eng Chem Res. 2013;52(30):10105-10113.

[17] Khan JA, Qasim M, Singh BR, Khan W, Das D, Naqvi AH. Polyaniline/$CoFe_2O_4$ nanocomposite inhibits the growth of Candida albicans 077 by ROS production. C R Chim. 2014;17(2):91-102.

[18] Kooti M, Kharazi P, Motamedi H. Preparation, characterization, and antibacterial activity of $CoFe_2O_4$/polyaniline/Ag nanocomposite. J Taiwan Inst Chem Eng. 2014;45(5):2698-2704.

[19] Xiong P, Huang H, Wang X. Design and synthesis of ternary cobalt ferrite/graphene/polyaniline hierarchical nanocomposites for high-performance supercapacitors. J Power Sources. 2014;245:937-946.

[20] Chen Z, Della Pina C, Falletta E, Lo Faro M, Pasta M, Rossi M, et al. Facile synthesis of polyaniline using gold catalyst. J Catal. 2008;259(1):1-4.

[21] Chen Z, Della Pina C, Falletta E, Rossi M. A green route to conducting polyaniline by copper catalysis. J Catal. 2009;267(2):93-96.

[22] Della Pina C, Falletta E, Lo Faro M, Pasta M, Rossi M. Gold-catalysed synthesis of polypyrrole. Gold Bull. 2009;42(1):27-33.

[23] Della Pina C, Falletta E, Rossi M. Conductive materials by metal catalyzed polymerization. Catal Today. 2011;160(1):11-27.

[24] Della Pina C, Rossi M, Ferretti AM, Ponti A, Lo Faro M, Falletta E. One-pot synthesis of polyaniline/Fe3O4 nanocomposites with magnetic and conductive behaviour. Catalytic effect of Fe3O4 nanoparticles. Synth Met. 2012;162(24):2250-2258.

[25] Zhao SY, Lee DK, Kim CW, Cha RG, Kim YH, Kang YS. Synthesis of magnetic nanoparticles of Fe_3O_4 and $CoFe_2O_4$ and their surface modification by surfactant adsorption. Bull Korean Chem Soc. 2006;27(2):237-242.

[26] Focke WW, Wnek GE, Wei Y. Influence of Oxidation-State, pH, and Counterion on the Conductivity of Polyaniline. J Phys Chem. 1987;91(22):5813-5818.

[27] Wei Y, Hariharan R, Patel SA. Chemical and Electrochemical Copolymerization of Aniline with Alkyl Ring-Substituted Anilines. Macromolecules. 1990;23(3):758-764.

[28] Lahiri P, Sengupta SK. Spinel Ferrites as Catalysts - a Study on Catalytic Effect of Coprecipitated Ferrites on Hydrogen-Peroxide Decomposition. Can J Chem. 1991;69(1):33-36.

[29] Wang H, Huang J, Ding LY, Wang C, Han Y. Controlled Preparation of Monodisperse $CoFe_2O_4$ Nanoparticles by a Facile Method. J Wuhan Univ Technol-Mater Sci Ed. 2011;26(2):258-262.

[30] Lutterotti L. Total pattern fitting for the combined size-strain-stress-texture determination in thin film diffraction. Nucl Instrum Methods Phys Res, Sect B. 2010;268(3-4):334-340.

[31] Salaneck WR, Liedberg B, Inganas O, Erlandsson R, Lundstrom I, Macdiarmid AG, et al. Physical Characterization of Some Polyaniline, (Phi-N)X. Mol Cryst Liq Cryst. 1985;121(1-4):191-194.

[32] Epstein AJ, Ginder JM, Zuo F, Bigelow RW, Woo HS, Tanner DB, et al. Insulator-to-Metal Transition in Polyaniline. Synth Met. 1987;18(1-3):303-309.

[33] Conwell EM, Duke CB, Paton A, Jeyadev S. Molecular-Conformation of Polyaniline Oligomers - Optical-Absorption and Photoemission of 3-Phenyl Molecules. J Chem Phys. 1988;88(5):3331-3337.

[34] Wolf JF, Forbes CE, Gould S, Shacklette LW. Proton-Dependent Electrochemical-Behavior of Oligomeric Polyaniline Compounds. J Electrochem Soc. 1989;136(10):2887-2891.

[35] Alavi S, Thomas S, Sandeep KP, Kalarikkal N, Varghese J, S. Yaragalla S. Polymers for Packaging Applications: CRC Press; 2014

[36] Stejskal J, Gilbert RG. Polyaniline. Preparation of a conducting polymer (IUPAC technical report). Pure Appl Chem. 2002;74(5):857-867.

[37] Kitani A, Yano J, Kunai A, Sasaki K. A Conducting Polymer Derived from Para-Aminodiphenylamine. J Electroanal Chem. 1987;221(1-2):69-82.

[38] Geniès EM, Penneau JF, Lapkowski M, Boyle A. Electropolymerisation Reaction-Mechanism of Para-Aminodiphenylamine. J Electroanal Chem. 1989;269(1):63-75.

[39] Smit J, Wijn HPJ. Ferrites: Philips Technical Library; 1959.

[40] Coey JMD. Magnetism and Magnetic Materials: Cambridge University Press; 2009.

[41] Hansen MF, Mørup S. Estimation of blocking temperatures from ZFC/FC curves. J Magn Magn Mater. 1999;203:214-216.

[42] Vázquez-Vázquez C, López-Quintela MA, Buján-Núñez MC, Rivas J. Finite size and surface effects on the magnetic properties of cobalt ferrite nanoparticles. J Nanopart Res. 2011;13(4):1663-1676.

[43] Batlle X, Labarta A. Finite-size effects in fine particles: magnetic and transport properties. Journal of Physics D-Applied Physics. 2002;35(6):R15-R42.

[44] Benitez MJ, Petracic O, Salabas EL, Radu F, Tuysuz H, Schuth F, et al. Evidence for core-shell magnetic behavior in antiferromagnetic Co_3O_4 nanowires. Phys Rev Lett. 2008;101(9):097206.

[45] Cullity BD, Graham CD. Introduction to Magnetic Materials. 2nd ed: IEEE Press-Wiley; 2009.

[46] Skomski R. Simple Models of Magnetism: Oxford University Press; 2008.

[47] Dunlop DJ, Özdemir Ö. Rock Magnetism: Cambridge University Press; 1997.

[48] Manova E, Kunev B, Paneva D, Mitov I, Petrov L, Estournes C, et al. Mechano-synthesis, characterization, and magnetic properties of nanoparticles of cobalt ferrite, $CoFe_2O_4$. Chem Mater. 2004;16(26):5689-5696.

[49] Ngo AT, Pileni MP. Nanoparticles of cobalt ferrite: Influence of the applied field on the organization of the nanocrystals on a substrate and on their magnetic properties. Adv Mater. 2000;12(4):276-279.

[50] Tauxe L, Mullender TAT, Pick T. Potbellies, wasp-waists, and superparamagnetism in magnetic hysteresis. Journal of Geophysical Research-Solid Earth. 1996;101(B1):571-583.

Table 1. Catalytic polymerization of AD by O_2 or H_2O_2. The superscripts 'unc' and 'OAC' refer to uncoated and oleic acid coated (OAC) $CoFe_2O_4$ NPs, respectively.

Uncoated $CoFe_2O_4$ NPs	O_2 as oxidant		H_2O_2 as oxidant	
$CoFe_2O_4$/AD (molar ratio)	Sample	Yield (%)	Sample	Yield (%) [a]
0	3^{unc}	0	7^{unc}	40
0.02	4^{unc}	59	8^{unc}	53 (13)
0.10	5^{unc}	70	9^{unc}	70 (30)
0.20	6^{unc}	74	10^{unc}	83 (43)
OAC $CoFe_2O_4$ NPs	O_2 as oxidant		H_2O_2 as oxidant	
$CoFe_2O_4$/AD (molar ratio)	Sample	Yield (%)	Sample	Yield (%) [a]
0	3^{OAC}	0	7^{OAC}	39
0.02	4^{OAC}	67	8^{OAC}	80 (41)
0.10	5^{OAC}	75	9^{OAC}	89 (50)
0.20	6^{OAC}	81	10^{OAC}	98 (59)

[a] The value in brackets is the catalytic yield only due to the $CoFe_2O_4$ NPs.

Table 2. IR and UV-Vis spectroscopic parameters of emeraldine salt (sample 1), leucoemeraldine (sample 2), and PANI/$CoFe_2O_4$ composites 6^{unc} and 11.

Sample	Q/B	λ_1 (nm)	ε_1 (M^{-1} cm^{-1})	λ_2 (nm)	ε_2 (M^{-1} cm^{-1})	$\varepsilon_1/\varepsilon_2$
1	1.1	316	1994	601	1096	1.82
2	0.29	275	2128	557	108	19.7
6^{unc}	0.76	300	6630	584	1913	3.46
11	0.99	316	1992	600	1092	1.82

Table 3. Magnetic parameters of OAC $CoFe_2O_4$ NPs and PANI/$CoFe_2O_4$ nanocomposites calculated from FC magnetization isotherms at 5 K.

Sample	M_{sat} [a,b] (emu/g)	M_{rem} [a] (emu/g)	M_{rem}/M_{sat}	H_c (kOe)	H_{cr} (kOe) [c]	H_{cr}/H_c
OAC $CoFe_2O_4$ NPs	37.1	27.1	0.73	18.5	20.0	1.1
5^{OAC}	58.9	14.3	0.24	8.7	18.7	2.1
6^{OAC}	57.8	28.4	0.49	14.5	18.3	1.3
9^{OAC}	109.6	27.2	0.25	8.2	19.1	2.3
10^{OAC}	88.6	35.7	0.40	13.5	19.3	1.4

[a] Mass magnetization M is referred to the NP mass (*not* composite mass). [b] M_{sat} is the magnetization at the maximum attainable field H = +50 kOe. [c] Calculated by the ΔM method.[50]

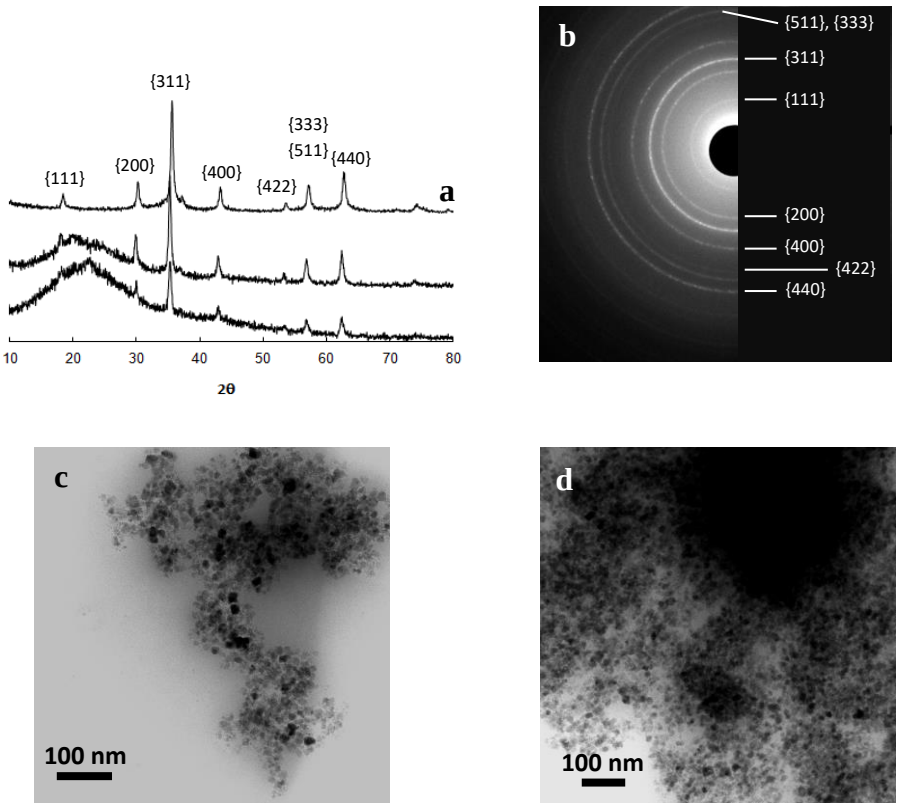

Figure 1. Diffractometry and morphology of pristine uncoated $CoFe_2O_4$ NPs and nanocomposites. (a) XRD patterns of pristine uncoated $CoFe_2O_4$ NPs (top), sample 9^{unc} (middle) and sample 10^{unc} (bottom). The peaks are labeled with reference to the spinel structure. (b) Electron diffraction and (c,d) TEM images of OAC $CoFe_2O_4$ NPs.

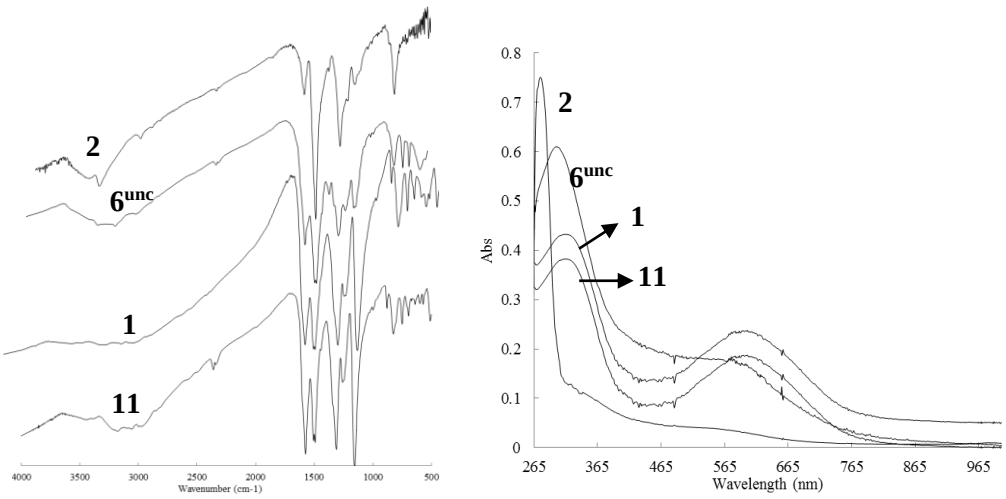

Figure 2. FT-IR and UV-vis spectra of samples: 6^{unc} (0.092 mM,), 2 (0.353 mM), 1 (0.217 mM) and 11 (0.087 mM,).

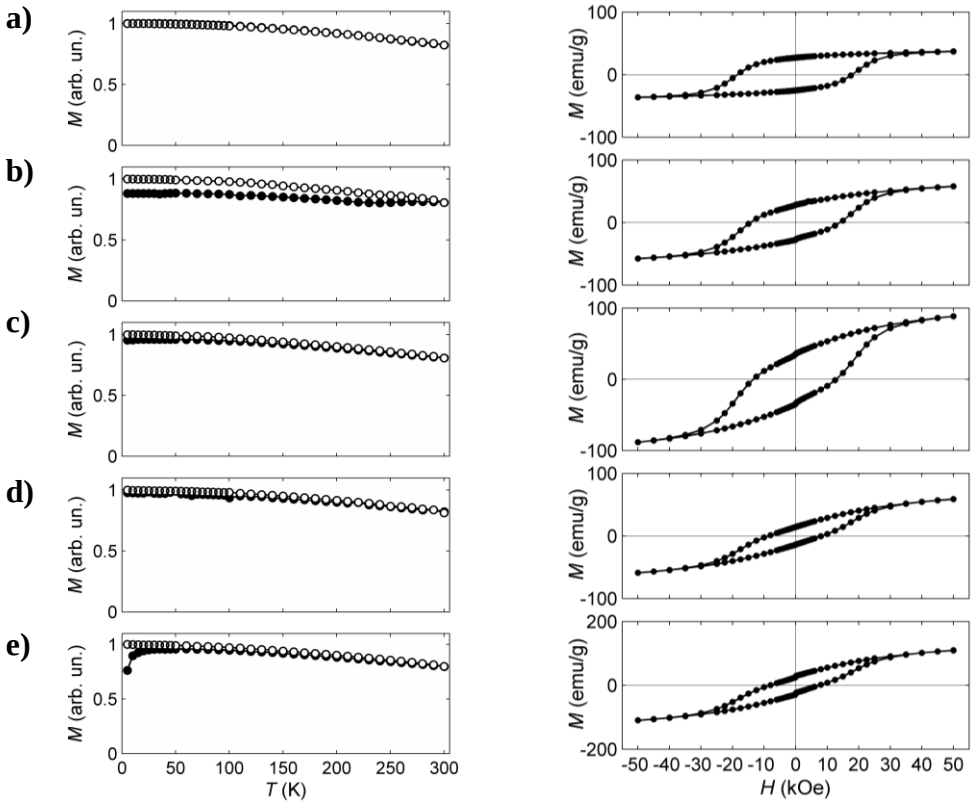

Figure 3. Magnetization of OAC $CoFe_2O_4$ NPs and PANI/$CoFe_2O_4$ nanocomposites. Left: ZFC (solid circles) and FC (hollow circles) magnetization; right: magnetization isotherms (FC, T = 5 K). a) OAC $CoFe_2O_4$ NPs, b) sample 6^{OAC}, c) sample 10^{OAC}, d) sample 5^{OAC}, e) sample 9^{OAC}.